**Supporting information**

# Different magnetic responses observed in $Co^{II}_4$, $Co^{II}_3$ and $Co^{II}_1$-based MOFs

Chao Zhang,[a] Zhong-Yi Liu,[a] Ning Liu,[a] Hong Zhao,[a] En-Cui Yang*[a] and Xiao-Jun Zhao*[a, b]

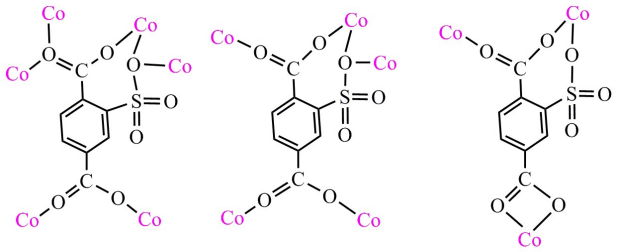

**Scheme S1** Binding modes of $stp^{3-}$ ligand in **1–4**.

**Table S1.** Selected bond lengths (Å) and angles (º) for **2** [a]

| | | | |
|---|---|---|---|
| Co(1)–O(1)$^{\#1}$ | 2.083(2) | Co(1)–N(3) | 2.031(2) |
| Co(2)–O(2) | 2.165(2) | Co(2)–O(3)$^{\#4}$ | 2.068(2) |
| Co(2)–O(5) | 2.182(2) | Co(2)–O(8) | 2.069(2) |
| Co(2)–O(8)$^{\#5}$ | 2.072(2) | Co(2)–N(1) | 2.085(2) |
| Co(3)–O(1)$^{\#6}$ | 2.224(2) | Co(3)–O(4)$^{\#7}$ | 2.014(2) |
| Co(3)–O(5)$^{\#5}$ | 2.305(2) | Co(3)–O(8) | 2.004(2) |
| Co(3)–O(9W) | 2.190(5) | Co(3)–N(2) | 2.059(2) |
| O(1)$^{\#1}$–Co(1)–O(1)$^{\#2}$ | 131.18(12) | N(3)–Co(1)–O(1)$^{\#1}$ | 99.95(9) |
| N(3)–Co(1)–O(1)$^{\#2}$ | 112.89(9) | N(3)$^{\#3}$–Co(1)–N(3) | 94.36(13) |
| O(2)–Co(2)–O(5) | 92.03(8) | O(3)$^{\#4}$–Co(2)–O(2) | 96.87(8) |
| O(3)$^{\#4}$–Co(2)–O(5) | 85.03(8) | O(3)$^{\#4}$–Co(2)–O(8)$^{\#5}$ | 97.12(8) |
| O(8)–Co(2)–O(2) | 83.10(8) | O(3)$^{\#4}$–Co(2)–N(1) | 93.08(9) |
| O(8)–Co(2)–O(5) | 92.39(8) | O(8)$^{\#5}$–Co(2)–O(5) | 79.62(8) |
| O(8)–Co(2)–O(8)$^{\#5}$ | 82.49(8) | O(8)–Co(2)–N(1) | 89.50(9) |
| O(8)$^{\#5}$–Co(2)–N(1) | 97.21(9) | N(1)–Co(2)–O(2) | 91.63(9) |
| O(4)$^{\#7}$–Co(3)–O(1)$^{\#6}$ | 98.32(8) | O(4)$^{\#7}$–Co(3)–O(5)$^{\#5}$ | 82.34(8) |
| O(4)$^{\#7}$–Co(3)–O(9W) | 81.98(15) | O(8)–Co(3)–O(1)$^{\#6}$ | 92.39(8) |
| O(8)–Co(3)–O(4)$^{\#7}$ | 96.82(8) | O(8)–Co(3)–O(5)$^{\#5}$ | 78.10(7) |
| O(8)–Co(3)–N(2) | 93.63(9) | O(9W)–Co(3)–O(1)$^{\#6}$ | 79.88(15) |
| O(9W)–Co(3)–O(5)$^{\#5}$ | 109.60(14) | N(2)–Co(3)–O(1)$^{\#6}$ | 100.04(9) |
| N(2)–Co(3)–O(5)$^{\#5}$ | 81.43(8) | N(2)–Co(3)–O(9W) | 90.18(15) |

[a] Symmetry codes: $^{\#1}$ $x$, $1 - y$, $z - 1/2$; $^{\#2}$ $-x$, $1 - y$, $-z$; $^{\#3}$ $-x$, $y$, $-1/2 - z$; $^{\#4}$ $1 - x$, $y$, $1/2 - z$; $^{\#5}$ $-x$, $-y$, $-z$; $^{\#6}$ $-x$, $y$, $1/2 - z$; $^{\#7}$ $-1 + x$, $-y$, $z - 1/2$.

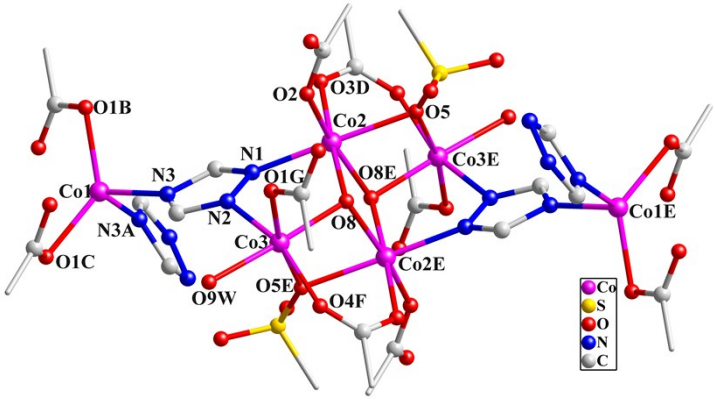


(a)

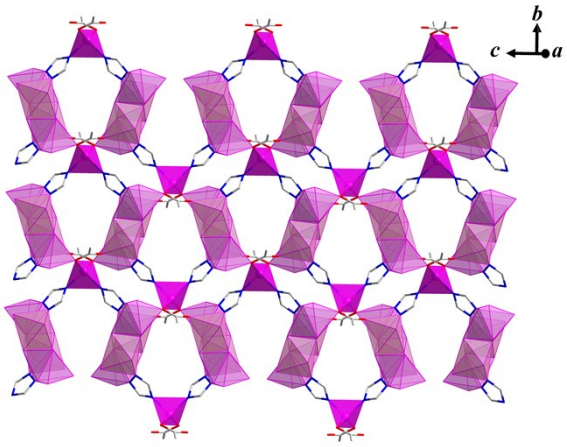


(b)

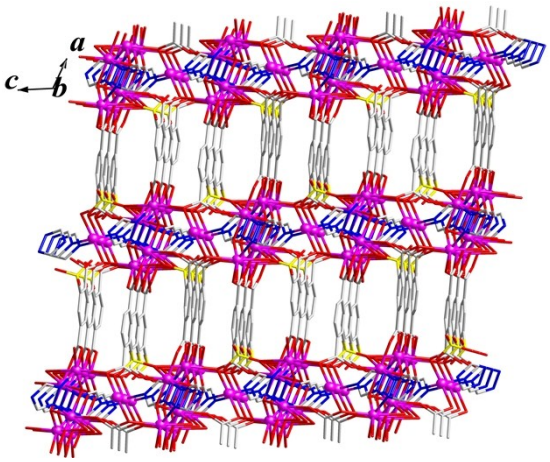


(c)

**Fig. S1** (a) Local coordination environments of $Co^{II}$ ions in **2** (H atoms were omitted for clarity. Symmetry codes: A = – *x*, *y*, –1/2 – *z*; B = *x*, 1 – *y*, *z* – 1/2; C = – *x*, 1 – *y*, – *z*; D = 1 – *x*, *y*, 0.5 – *z*; E = –*x*, – *y*, – *z*; F = *x* – 1, – *y*, *z* – 1/2). (b) 2D layer of **2** constructed from $\mu_3$-trz$^-$ extended $Co^{II}_4$ and $Co^{II}_1$ subunits. (c) Pillared-layer framework of **2**.

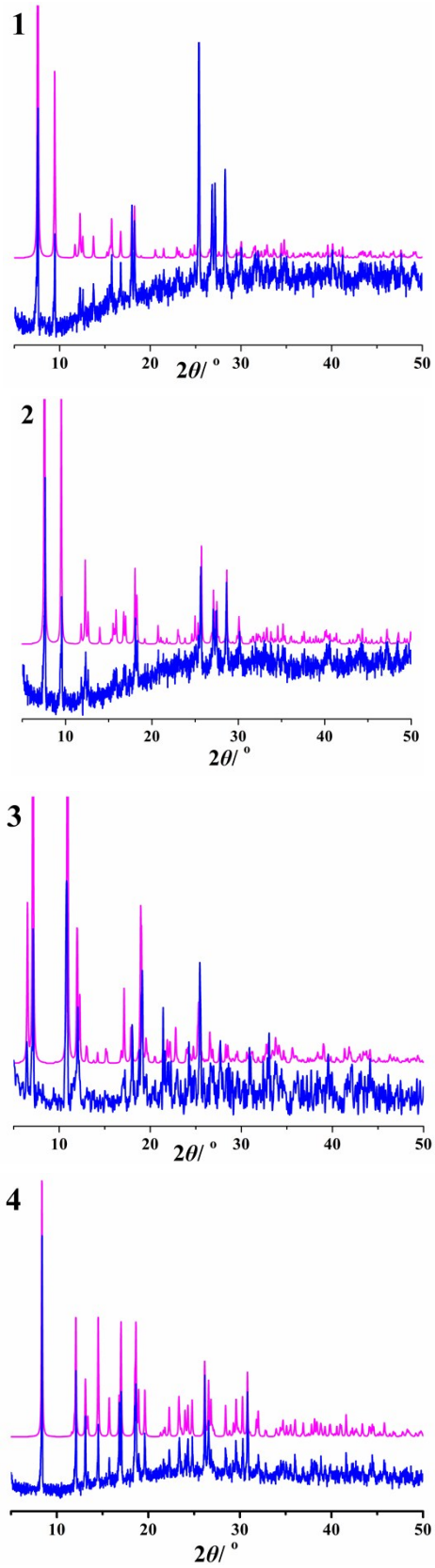


**Fig. S2** Simulated (purple) and experimental (blue) X-ray powder diffraction patterns for **1–4**.

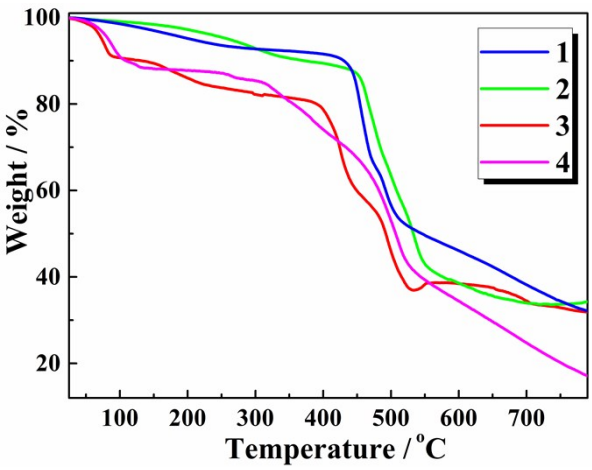


**Fig. S3** TG curves for **1**–**4**.

**Table S2.** Geometric parameters (Å, deg) for the sununit of **1**

| Pathway | Linkages | $r_{Co\cdots Co}$ | ∠CoOCo |
|---|---|---|---|
| $J_1$ | $\mu_3$-OH$^-$<br>$\mu_3$-OH$^-$ | 3.1501(3) | 98.356(6) |
| $J_2$ | $\mu_3$-OH$^-$<br>–NN– | 3.4409(4) | 114.638(7) |
| $J_3$ | $\mu_3$-OH$^-$<br>Single atom bridging sulfonate | 3.2183(4) | 104.355(6)<br>91.189(5) |
| $J_4$ | Single atom bridging carboxylate | 3.8788(4) | 123.704(98) |
| $J_5$ | $\mu$-*syn*, *anti*-COO$^-$ | 4.3416(4) | |

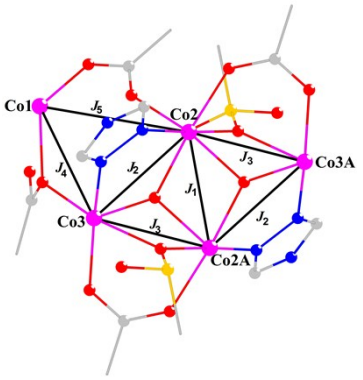

**Table S3.** Geometric parameters (Å, deg) for the sununits of **3**

| Pathway | Linkages | $r_{Co\cdots Co}$ | ∠CoOCo | |
|---|---|---|---|---|
| $J_1$ | $\mu_3$-OH$^-$<br>$\mu_3$-OH$^-$ | 3.1723(18) | 98.3(2) | 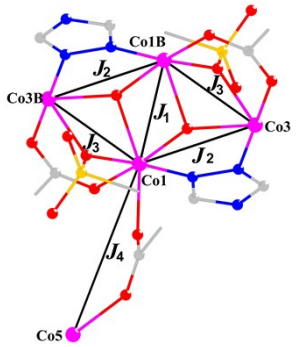 |
| $J_2$ | $\mu_3$-OH$^-$<br>–NN– | 3.5371(18) | 117.4(3) | |
| $J_3$ | $\mu_3$-OH$^-$<br>Single atom bridging sulfonate | 3.2177(15) | 101.1(2)<br>89.6(2) | |
| $J_4$ | *μ-syn*, *anti*-COO$^-$ | 5.3418(25) | | |
| $J_1$ | $\mu_3$-OH$^-$<br>$\mu_3$-OH$^-$ | 3.1766(18) | 98.1(2) | 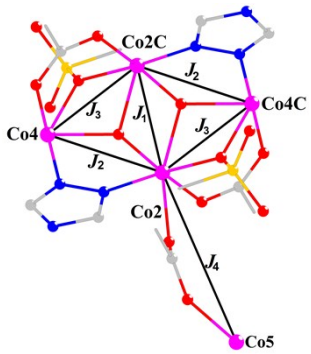 |
| $J_2$ | $\mu_3$-OH$^-$<br>–NN– | 3.5584(18) | 117.7(3) | |
| $J_3$ | $\mu_3$-OH$^-$<br>Single atom bridging sulfonate | 3.2169(15) | 101.1(3)<br>89.8(2) | |
| $J_4$ | *μ-syn*, *anti*-COO$^-$ | 5.3484(25) | | |

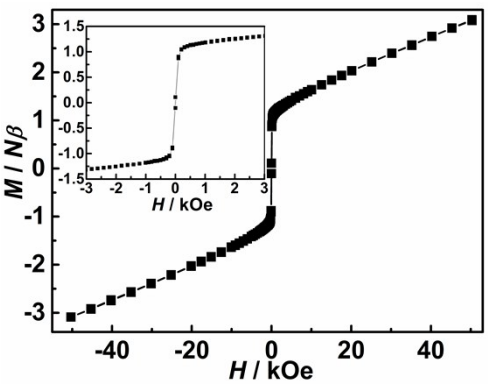


**Fig. S4** Magnetic hysteresis loop for **1** measured at 2.0 K.